



Crashworthiness Characteristic of Glass Fibre Reinforced Polymer (GFRP) Composite Tubes Under Quasi Static Loading

Muhammad Fareq Ikhwan As'ari, Alif Zulfakar Pokaad^(✉), and Logah Perumal

Faculty of Engineering and Technology, Multimedia University Melaka, Jalan Ayer Keroh
Lama, 75450 Bukit Beruang, Melaka, Malaysia

alif.pokaad@mmu.edu.my

Abstract. The overarching goal of this final year project are to design and fabricate a composite glass fibre reinforced with three different types of polymers (epoxy, polyester, and vinyl ester) followed by studying the crashworthiness characteristic under quasi – static load by using a universal testing machine. The composite specimens were fabricated by applying the hand layup technique by using woven glass fibre reinforced with the mentioned polymers as a resin. The crashworthiness characteristic of the composite tubes were evaluated by measuring the peak load, mean load, specific energy absorption, total energy absorption, and crush force efficiency with an addition of their fabrication costs. The failure mode and behavior of the tubes were studied and analyze by taking pictures of each crushed specimens and recording of their load–displacement curves when conducted the compression test. There were two types of failure mode identified through out the study on the specimens either local buckling or lamina bending. The vinyl ester composite was identified to be the most desirable since it gives the highest peak load, mean load, total energy absorption, specific energy absorption, and crush force efficiency values when compared to the other type of composite polymers. However, it was found that polyester had the lowest fabrication cost needed among the others. The whole project was successfully completed without any minor or major accident along the process from beginning until the completion.

Keywords: composite tube · polyester · vinyl ester · epoxy

1 Introduction

An improvement of materials has been widely studied in most of industry especially for manufacturing, their research and development department had given an attention on absorption and strength of materials as well as low cost of production. In automotive industry, with an increased in the number of vehicle crashworthiness, manufacturers and researchers have put an effort in performing experimental research and providing a theoretical design in depth for the mechanic of crumpling. This dedicated study provides a fundamental knowledge and idea to the engineers in designing a vehicle passenger

material with the maximum amount of energy will dissipate throughout deformation process on the material, thus protecting passengers inside the vehicle [1].

The main idea for an improvement is mainly focus on the crashworthiness of the vehicle structure. This can be achieved by improving on a certain constraint such as reducing transmission of force and deformation. Normally, the development of deformation is relied on the total energy dissipated through their structure and geometry components. Usually, this happened on their frames and design sections or in their thin wall for tubes shapes. This energy absorption is dependent on the types of crushing modes and materials, it is clearly given different results for every component used [1].

Due to this reason, investigation was done on the several crashworthiness parameters, with major attention being taken on the type of geometry behaviour. This includes of their process of fabrication, tube cross sectional, fibre arrangement and sequence for laminating stacking, triggering mechanism and wall thickness. Therefore, these will result to a lot of improvement in terms of their weight, strength and stablization of the composite tubes [2].

Therefore, this paper is focusing on the study of energy absorption characteristics on Glass Fibre reinforced with different type of polymers; epoxy, vinyl ester and polyester. These polymers used will provide as an improvement on their mechanical properties. For each type of fabricated composites will produce amount of energy absorbed and this will be taken to be measure and analysed. At the end of the project, results of this research will disclose all the set of energy absorption data respect to the type of polymers accordingly.

2 Mechanism and Modes of Crushing

In these days, crashworthiness for automotive parts by using composites (laminate) are very demanding because a lot of energy absorption can be absorbed during vehicle crash [3]. Nowadays, for luxury automotive vehicles, they had replaced aluminium and steel into composite material based on the research done on crash element for this material [4]. Due to high strength and toughness on composite material, they had been used mostly for structure that need an improvement on their crashworthiness [5]. In addition, they are also providing almost the same production cost compared to common materials used [6]. Their impact behaviour seems show a positive result; thus, this composite is highly resistance for wear, shock, impact, static and dynamic as well as low in a corrosion [7]. This is the main reason they are only used for any improvement needed for high impact strength [8]. The crushing mode analysis will be determined as part of their material energy absorption capability.

In the previous study and research, the mode of crushing can be classified into several classification such as, transverse shearing, lamina bending, brittle fracturing and local buckling. In Fig. 1 shown four types of classified crushing modes.

2.1 Transverse Shearing

Transverse shearing is one of the classifications of mode of crushing, it is recognized by having wedge shaped laminate cross section with one or more short interlaminar and

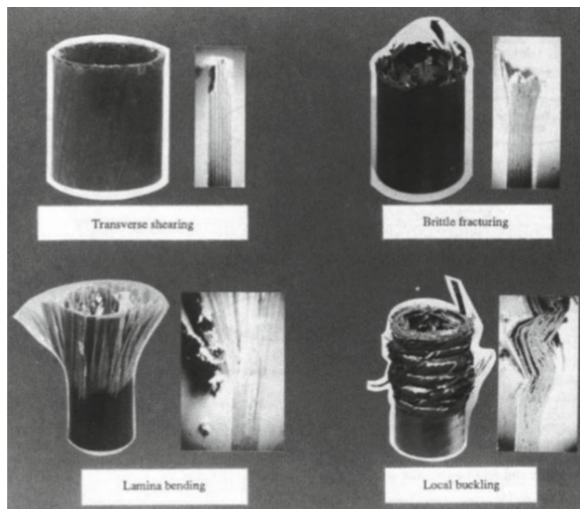


Fig. 1. Types of classified crushing modes [9]

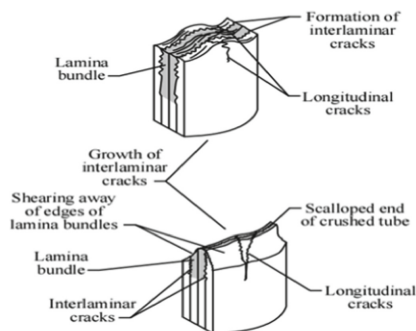


Fig. 2. Transverse shearing crushing mode [9].

longitudinal cracks. This gives an impact in the formation of incomplete lamina bundles in laminate as shown in Fig. 2. This type of crushing mode usually known by having high modulus, low failure strain graphite epoxy tubes [10]. Other than that, this also happened for 90-degree graphite epoxy and glass epoxy tubes [11]. This transverse shearing can be demonstrated in tubes reinforced with brittle fibres. As shown in Fig. 2 is the primary energy absorption process that involves the fracture of the lamina bundles. The lamina bundles serve as columns, which can withstand the applied load. This described how interlaminar cracks spread until the sides of the column are fractured because of the application of load. This results in a wedge-shaped cross section of the column [9].

2.2 Lamina Bending

As seen in Figs. 1 and 3, the interlaminar, intralaminar, and parallel to fibre cracks in the lamina bending crushing mode are exceedingly long, although the lamina bundles do not

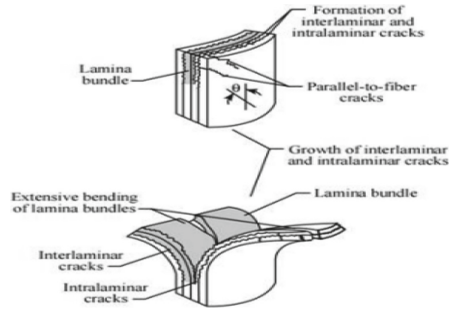


Fig. 3. Lamina bending crushing modes [9]

fracture in this mode. A great number of research [12–16] have evaluated materials that exhibit a lamina bending crushing mode. The main energy absorption can be described when there is development of matrix cracks during the crushing mode happened.

For the specimens that have a lamina bending crushing mode, there will be a friction occur as their secondary energy absorption processes [16–18]. Once it starts to bend, the lamina bundles will slide through the loading surface. This is where the friction mechanism exists, when the relative motion of adjacent lamina slides into each other but in extended, these friction effects is not being recognised.

2.3 Brittle Fracturing

The fusion of the transverse shearing and lamina bending crushing modes is described as brittle fracturing crushing mode. Commonly, for this mode of crushing, it usually happened for brittle fibre reinforced composite tubes that have brittle fracture crushing mode [4–12]. Figures 1 and 4 show the commonalities among the modes, which include interlaminar and longitudinal cracks, a scalloped crushing surface, and the primary energy absorption mechanism. The lamina bundles will bend, and fracture will occur at their bottom part if the brittle fracturing mode is allowed. There will be load pass through inside the specimens once the lamina bundle undergoes fracturing. Lastly, the process are repeated again starting from crack development, bending of lamina bundle, and fracture until the crack is developed completely [3].

2.4 Local Buckling

In terms of strength and ductility, regardless of their type of materials failure either ductile or brittle, they will result to local buckling mode on the fiber reinforced composite materials. As shown in Fig. 1 and 5, these are examples of local buckling happened as their crushing mode. There are plastically deform identified at somewhere at the buckle area during the compression zone specifically for ductile fibre reinforced composite. Besides that, there are a possibility fracture occur on the during the side tension of buckling. Once crushing process is completed, the composite will maintain their integrity structure, and during post crushing, this will be used to present as an experiment result.

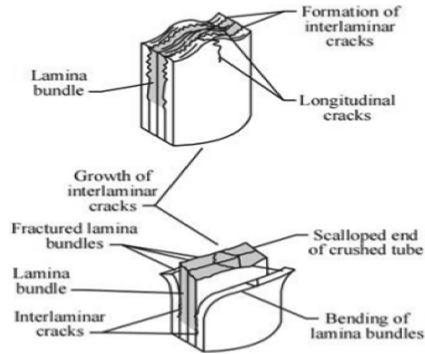


Fig. 4. Brittle fracturing crushing modes [9]

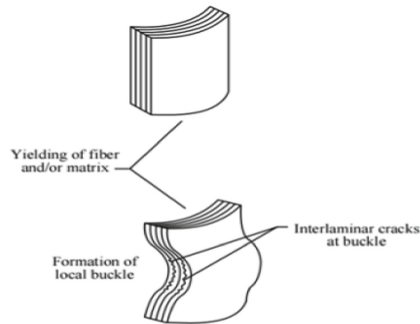


Fig. 5. Local buckling crushing modes [9]

Therefore, when in high stress conditions, the plastic deformation will occur, this is due to the percentage failure strain of the fibre is lower compared to the matrix used [4]. For brittle fibres, the plastic stress strain is not existed. This is because of high failure strain matrix had prevented appearance of the interlaminar fractures. As shown in Fig. 5, the interlaminar cracks develop somewhere at the area of the buckles take place in the local buckling. Usually, this local interlaminar cracks are not develop to the nearby buckles [3].

2.5 Crashworthiness Formula

The integrity of the structure is determined by study their crashworthiness parameter. Besides that, the energy absorption are take into a concern based on the failure modes identified. The energy impact is absorbed during the compression testing while it was set to move in a steady mode in the profile load. A typical load-displacement graph, as shown in Fig. 6, can be used to describe the crashworthiness characteristics. There are three major different phases occur during this compression testing. Pre crushing is the first phase occur which represent the material is start to fail. This followed by the second phase which is known as post crushing, in this phase, the extending failure of the specimen is happened and represent as average in the crushing load. Lastly, at this third

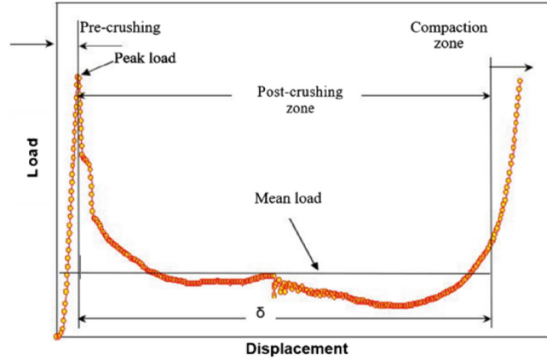


Fig. 6. Load vs displacement graph [19]

phase, the load is start to rise during the compression of the specimen until completion of the test. Here are some of the important crashworthiness parameters can be identified, this includes of the initial peak load (P_{max}), the total energy absorption, the maximum displacement, the average crushing load, the specific energy absorption (SEA), and the crushing force efficiency (CFE).

2.5.1 Peak Load (P_{max})

During pre crushing and the starting phase, the maximum load reached in the load displacement graph is known as peak load. This represents as the maximum amount of load that specimen can handled before it starts to deform.

2.5.2 Mean Load (P_m)

Mean load is calculated by averaging the total crushing load across the full length of the deformation in the post-crushing zone.

$$P_m = \frac{\int_0^{\delta_f} P d\delta}{\delta_f} \quad (1)$$

Mean crushing load is noted as P_m , the total force applied on the specimen in function of $P(\delta)$, and δ_f represents the final crush distance is known as P .

2.5.3 Total Energy Absorption (E_a)

Area calculated under the load displacement graph, also known as the total work done, may be used to determine the total energy absorbed of the specimens. At the end, the total energy absorbed may be computed as follows:

$$E_A = \int_0^{\delta_f} P d\delta \quad (2)$$

Where F is the crush force in axial direction, δ is the displacement and δ_f is the final displacement in ikaxial direction. It should be emphasized that elastic return is not

considered here. Total energy absorption is represented by the area under the axial force versus axial displacement curve.

2.5.4 Specific Energy Absorption (SEA)

The energy absorption per unit mass, also known as specific energy absorption, *SEA*, is important when evaluating or comparing energy absorption capabilities for various types of materials when weight is a factor. It is defined as the total energy absorbed per unit mass and is computed as follows.

$$SEA = \frac{E_A}{m} \quad (3)$$

Where *SEA* is the energy absorbed per unit mass (kJ/kg), and *m* is the mass of the specimens used (kg).

2.5.5 Crushed Force Efficiency (CFE)

The crush force efficiency, CFE, is another parameter to determine the best energy absorption material. This can be determining the specimen performance through the calculation of ratio between mean load and peak load. Noted that, for CFE value approaching to unity or higher, this indicates a steady progression of the specimens tested. In mathematically CFE formula as follows:

$$CFE = \frac{P_m}{P_{max}} \quad (4)$$

Where CFE is the crush force efficiency, *P_m* is the mean crushing load (kN), and *P_{max}* is the maximum load.

3 Methodology

3.1 Experimental Process Flow Chart

See Fig. 7.

3.2 Specimen Preparation

In designing this experimental project, it started with determine all the variables and specifications of the specimens, this includes of their length, diameter, and geometry of the composite tube. This is to ensure that the specimens shall meet the maximum load capacity of the testing machine and to avoid any problems rise during the whole process of experiment. Thus, the dimensions of the composite tubes are set to be design and fabricate as a circular shape tube with a cutting length of 100 mm and outer diameter of 32 mm for every specimen prepared.

The process flow shall be proceeded to next step once all the variables and specifications are confirmed. The method use in this fabrication process is hand layup technique

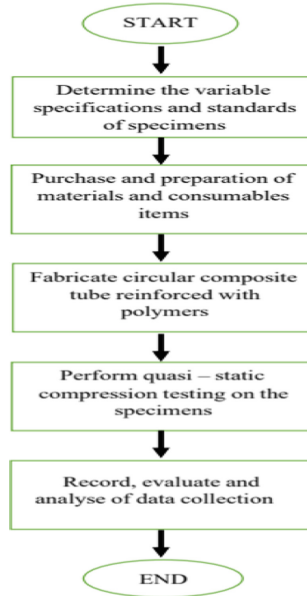


Fig. 7. Experimental process flow chart

which is the most common practice in the industry and well known as a simple and low-cost process. The most essential materials needed to complete this fabrication process are glass fibre is composite part and three different types of polymers resins which are Epoxy, Polyester, Vinyl Ester, and hardener. These shall be purchased and prepared before fabrication process take place.

Next, is the fabrication of this circular composite tubes reinforced with the polymers, the number of woven glass fibre plies used are kept constant with the number of three plies of winding each of the polyvinyl chloride (PVC) which is act as a mould tubes. There are three tubes in total with the overall length of 100 mm and was identical in every way.

The final stage of this entire experimental process is compression testing, all specimens shall undergo a quasi – static load compression test to determine its crashworthiness. Lastly, collected data are being tabulated to plot a graph between load and displacement in relation to time by using a software as well as calculated their crashworthiness parameter.

As per supplier recommendations and technical info, the mixing weight ratio for epoxy and hardener are set to 2:1. Meanwhile, for polyester and vinyl ester mixed with hardener with a weight ratio of 2% of total amount of polymer used. Then the stirring process is needed for about 7 to 10 min before it can be utilized. The mixture was distributed uniformly on the woven glass fabric as shown in Fig. 8(a) and distributed using a scrapper.

Then the fabric was wrapped around a PVC tube as shown in Fig. 8(b). The wire tape was used to put on pressure on the wrapped fabric as well as to remove excess polymer resin as shown in Fig. 1(c). Upon completion of curing process after about 24 h, the

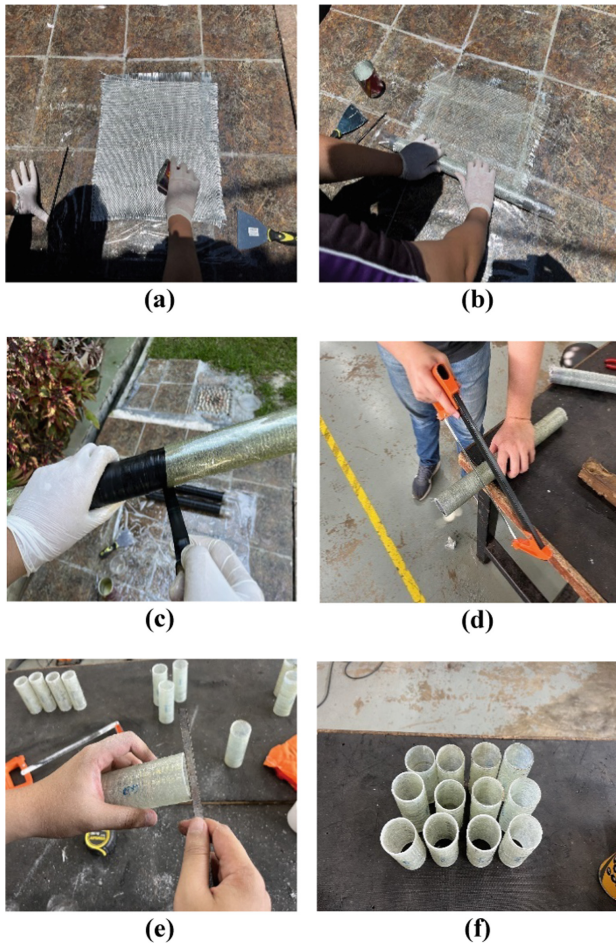


Fig. 8. Process of hand layup technique

composite tubes were cut into desired pieces using handback saw as shown in Fig. 8(d) followed by filing both end of the composite tubes by using chisel Fig. 8(e). The final product of the specimens is shown in Fig. 8(f).

3.3 Quasi Static Compression Test

The fabricated specimen's tube was subjected to compression tests using a universal testing machine model INSTRON 3367 with a load capacity of 30 kN. The speed was set at a constant cross head of 5 mm/min for the entire quasi – static load compression testing. This quasi – static axial compression test was performed to evaluate the crash-worthiness parameters of the fabricated composite tubes. The ASTM D7136 guidelines were followed while conducting this testing.

The machine was setup specifically for hollow circular tubes specimens by the lab technician. The final composite specimen tube was placed in between top and bottom plater before it was crushed. The bottom plate was set to be in a static, while the top plate was move steadily downwards which had been pre set before the compression start. During the compression test, video and photo are being taken for the purpose of analysis.

4 Results and Discussion

4.1 Trend in Load Extension for Epoxy

In this part, each of the crushing trend curve for epoxy specimens were illustrated in Fig. 9. In comparison, there were some different on the shape of the curve plotted for each of the epoxy specimens. This was happened due to during hand layup under surface finishing process, the edge of each of the specimens were not filed and flatten accordingly. Thus, it was expected to be happened on the crushing trend curve. In overall, the similarity for all the three-load extension curve was the curve linearly increase during this pre crushing phase until it reached the peak load. This occurred in between of 0 to 5 mm displacement. After that, the value of the load start to decreases significantly before the curve start to change in the trend during last phase of post-crushing. All the specimens shown that there was insignificant fluctuation for the remaining extension displacement throughout the post-crushing phase (Fig. 10).

4.2 Trend in Load Extension for Polyester

The trend in load extension for the three set of Polyester specimens is shown in Fig. 11. The load extension trend for all specimens shows a similarity in term of their shape developed throughout the whole crushing process. The range for peak load for all the three specimens is ranging between 15000 to 20000 N, (N) and this happened in between 10 to 30 mm displacement. The value of declined load happened at 70 to 80 mm displacement for all the specimens, whereby the load is below 10000 N, (N) before it started to ascend gradually in the curve at the end of the crushing testing. This clearly described that the whole length of the specimens has been deformed and crushed completely under quasi – static load testing (Fig. 12).

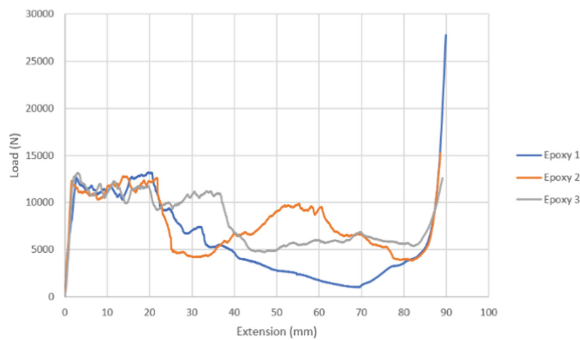


Fig. 9. Load extension curve for epoxy

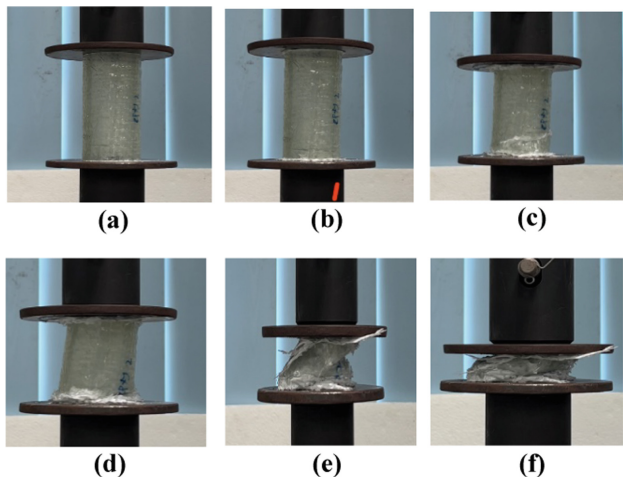


Fig. 10. Crushing stages. (a) At 0 mm (b) At 10 mm (c) At 30 mm (d) At 50 mm (e) At 60 mm (f) At 80 mm displacement.

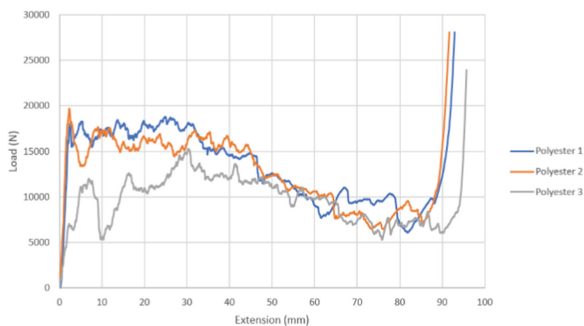


Fig. 11. Load extension curve for polyester

4.3 Trend in Load Extension for Vinyl Ester

The trend in load extension curve developed for vinyl ester for each of the specimens are varies. As for Fig. 13 shows that the shape of curve developed from the quasi – static testing are almost identical. The highest peak load for both specimen number one and three were reached at 20 mm displacement. In addition, the curved gradually increase at this point before both of it started to decline after 30 mm displacement and continue to gradually rise at a displacement of 80 mm onwards where the compaction phase began. At this place, the load is reaching their second peak load at 30000 N. In some difference, it can be seen clearly that both of it have unidentically in the amount of peak load produce during 20 mm displacement.

As for Fig. 13 specimen number two, the load extension curve developed starting from the beginning of displacement took place and continue gradually until the end of the crushing stages, where it started to have it highest peak at 95 mm displacement with

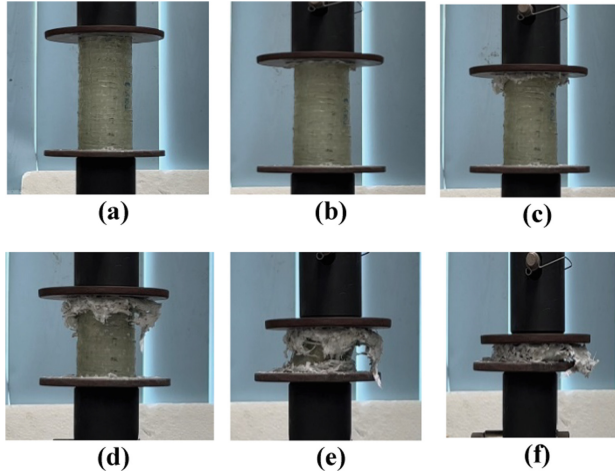


Fig. 12. Crushing stages. (a) At 0 mm (b) At 10 mm (c) At 30 mm (d) At 50 mm (e) At 60 mm (f) At 80 mm displacement.

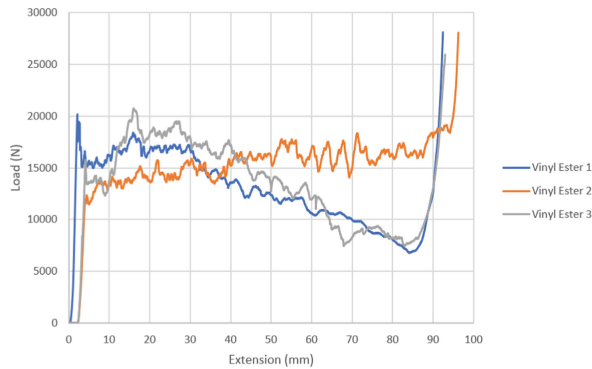


Fig. 13. Load extension curve for vinyl ester

the amount of load around 25000 N which at the phase of compaction and completion of deformation on crushing stages (Fig. 14).

4.4 Crashworthiness Parameter

Crashworthiness on the composite structure is access retrospectively by analyzing all the necessary parameters, oftenly on their peak load, mean load, total energy absorption, specific energy absorption, and crush force efficiency. The other most important parameter that must be considered is the costing. This is to determine and compare between their crashworthiness parameter and the cost effectiveness for the composite structure to be chosen and accepted as an alternative material in the industry. In Table 1 shown is a summarization for all the parameters mentioned earlier. Noted that the tabulated data

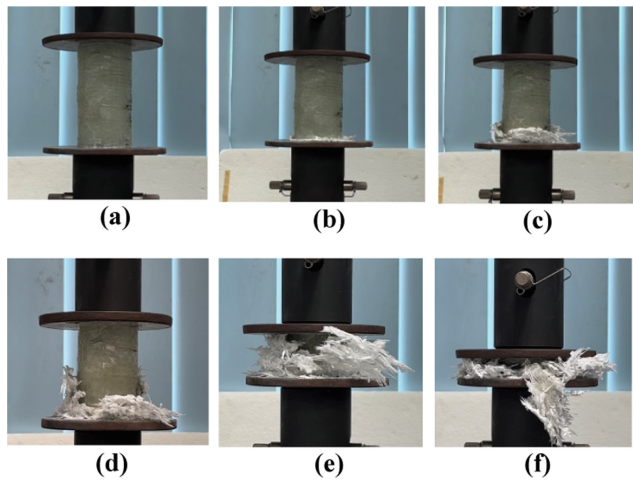


Fig. 14. Crushing stages. (a) At 0 mm (b) At 10 mm (c) At 30 mm (d) At 50 mm (e) At 60 mm (f) At 80 mm displacement.

Table 1. Crashworthiness parameter of all type of composite materials

Specimen	Total energy absorption Ea (kJ)	Specific Energy Absorption, SEA (kJ/kg)	Mean Load Pm (kN)	Peak Load $Pmax$ (kN)	Crush Force Efficiency, CFE	Fabrication cost, RM
Epoxy	0.6505	13.8199	7.2591	18.401	0.3964	74.50
Polyester	1.1081	26.4593	11.8655	26.441	0.4488	29.50
Vinyl Ester	1.2948	31.8782	13.7985	27.154	0.5082	41.52

shown are the average value of each of the specimens from different type of polymers fabricated in the composite.

Based on the crashworthiness parameter results achieved, it clearly shown that vinyl ester had the highest value for all the parameter studied in this paper. The crush force efficiency, CFE value for vinyl ester gave the nearest to the unity value, which shows that this is the best type of polymer to be considered in designing the vehicle structure components. In addition, the different and huge gap of the CFE value from unity shows that there is a sudden change in deceleration, thus in designing a vehicle structure, this type of polymer should not be considered. For the SEA value, the higher the value, indicate that energy absorber are very efficient, in this case, vinyl ester has the highest SEA value compared to epoxy and polyester.

5 Conclusion

This experimental study was conducted to identify the effects of crashworthiness on the glass fibre reinforced with different type of polymers (epoxy, polyester, and vinyl ester) composite tubes. This covered the crushing modes failure and crashworthy parameter occurred. Hand layup technique was introduced and performed to fabricate this composite tubes. Then, all the fabricated specimens were tested under quasi static load. Based on the results achieved from the experiment. By using vinyl ester as a reinforcement polymer is the most effective and give the highest value of all crashworthiness parameters compare to epoxy and polyester. Thus, this vinyl ester provides an excellent energy absorption capability and can be selected as the most appropriate polymers for energy absorbing materials.

Acknowledgments. Sincere appreciation and thank you to Faculty of Engineering and Technology, Multimedia University Melaka, for providing all the sources and equipments throughout the process of completing my research.

References

1. A. G Mamalis, M. Robinson, D. E. Manolacos, G. A. Demosthenous, M. B. Ioannidis and J. Carruthersb, "Crashworthy capability of composite material structures," *composite structure* 37, pp. 109–134, 1997. DOI: [https://doi.org/10.1016/S0263-8223\(97\)80005-0](https://doi.org/10.1016/S0263-8223(97)80005-0)
2. A.B.M. Supian, S.M. Sapuan, M.Y.M. Zuhri, Z.E Syams and H. Hj. Ya, "Hybrid Reinforced Thermoset Polymer Composite in Energy Absorption Tube," *Defence Technology*, pp. 1–50, 2018. DOI: <https://doi.org/10.1016/j.dt.2018.04.004>
3. A.B.M. Supian, S.M Sapuan, M.Y.M Zuhri, E.S. Zainudin, H.H. Ya, H.N. Hisham, "Effect of winding orientation on energy absorption and failure modes of filament wound kenaf/glass fibre reinforced epoxy hybrid composite tubes under intermediate-velocity impact (IVI) load," *Materials Research and Technology* , vol. 1, pp. 1-14, 2020. DOI: <https://doi.org/10.1016/j.jmrt.2020.11.103>
4. Zhang, Yong, Xiang Xu, Shuran Liu, Tengting Chen, and Zhongwei, "Crashworthiness Design for bi-Graded Composite Circular Structures.," *Construction and Building Materials*, vol. 168, pp. 633-649, 2018. DOI: <https://doi.org/10.1016/j.conbuildmat.2018.02.159>
5. Pety, Stephen J., Jia En Aw, Anthony C. Gendusa, Philip R. Barnett, and R Scott, "Effect of Microchannel on the Crashworthiness of Fiber Reinforced Composites," *White Composite Structures*, vol. 184, pp. 428–436, 2018. DOI: <https://doi.org/10.1016/j.compstruct.2017.09.105>
6. Fazita, M. R. Nurul, H. P. S. Abdul Khalil, A. Nor Amira Izzati, and Samsul Rizal, "3 - Effects of Strain Rate on Failure Mechanisms and Energy Absorption in Polymer Composites," *Wood Head Publishing Series in Composites Science and Engineering*, pp. 51–78, 2019. DOI: <https://doi.org/10.3390/polym12061222>
7. Xin, Zhibo, Yugang Duan, Jin Zhou, and Hong Xiao, "Effect of Tailored Plies on the Energy Absorption Capability of Square CFRP Tubes with Discontinuous Fibers," *Composite Structures*, vol. 209, pp. 150-159, 2019.
8. Xiao, Lin, Guanhui Wang, Si Qiu, Zhaoxiang Han, and Dongxing Zhang, "Exploration of Energy Absorption and Viscoelastic Behavior of CFRPs Subjected to low Velocity Impact.," *Composites Part B: Engineering*, vol. 165, pp. 247-254, 2019. DOI: <https://doi.org/10.1016/j.compositesb.2018.11.126>

9. Farley, Gary L and Jones, Robert M, "Crushing Characteristic of Continuos Fiber Reinforced Composite Tubes," *Composite Material* , vol. 26, no. 1, pp. 37–50, 1992. DOI: <https://doi.org/10.1177/002199839202600103>
10. Farley, Gary L., and Robert M. Jones, "Energy-absorption capability of composite tubes and beams," Ph.D. Thesis, 1989.
11. Bannermann, D. C., and C. M. Kindervater, "Crash energy absorption properties of composite structural elements," *High performance composite materials; New applications and industrial products*, pp. 155–167, 1983.
12. Thornton, P. H., "Energy Absorption in Composite Structures," *J. Compos. Mater.*, vol. 13, pp. 247–262, 1979. DOI: <https://doi.org/10.1177/002199838201600606>
13. Price, J. N and Hull, D.v., "The Crush Performance of Composite structure," *Composite Structures*, E. J. Marshall, ed., Elsevier, p. 2.32–2.44, 1987.
14. Gunwan, Dheeraj., "Stress Concentration Studies in Flat Plates with Rectangular Cut-Outs using Finite Element Method," *International Journal of Mathematical, Engineering and Management Sciences*, vol. 1, no. 4, pp. 66–76, 2019. DOI: <https://doi.org/10.33889/IJMEMS.2019.4.1-006>
15. Ganesh Gupta K, Avadesh Yadav, Mritunjay Maharudraya Hiremath, Rajesh Kumar Prusty, Bankim Chandra Ray, "Enhancement of mechanical properties of glass fiber reinforced vinyl ester composites by embedding multi-walled carbon nanotubes through solution processing technique," *Elsevier* , vol. 1, pp. 1-6, 2020. DOI: <https://doi.org/10.1016/j.polymertesting.2020.107008>
16. Oshkovr, S. A., et al, "Crashworthiness characteristics investigation of silk/epoxy composite square tubes," *Composite Structures*, vol. 94, no. 8, pp. 2337–2342, 2012.
17. Keller, Thomas, "Overview of fibre-reinforced polymers in bridge construction," *Structural engineering international*, vol. 12, no. 2, pp. 66–70, 2002.
18. Mallick, P.K., "Materials, Manufacturing, and Design," *Mechanical Engineering* (Marcel Dekker, Inc.), vol. 83, pp. 74–81, 2007.
19. Alkbir, M.F.M., Sapuan, S.M., Nuraini, A.A. and Ishak, M.R., "Effect of geometry on crashworthiness parameters of natural kenaf fibre reinforced composite hexagonal tubes," *Materials & Design*, vol. 60, pp. 85–93, 2014.

Open Access This chapter is licensed under the terms of the Creative Commons Attribution-NonCommercial 4.0 International License (<http://creativecommons.org/licenses/by-nc/4.0/>), which permits any noncommercial use, sharing, adaptation, distribution and reproduction in any medium or format, as long as you give appropriate credit to the original author(s) and the source, provide a link to the Creative Commons license and indicate if changes were made.

The images or other third party material in this chapter are included in the chapter's Creative Commons license, unless indicated otherwise in a credit line to the material. If material is not included in the chapter's Creative Commons license and your intended use is not permitted by statutory regulation or exceeds the permitted use, you will need to obtain permission directly from the copyright holder.

